Evolution of structure in thin microcrystalline silicon films grown by electron-cyclotron resonance chemical vapor deposition

M. Birkholz,[a] B. Selle, E. Conrad, K. Lips, and W. Fuhs
Hahn-Meitner-Institut, Silizium Photovoltaik, Kekuléstr. 5, D-12489 Berlin, Germany

(Received 28 March 2000; accepted for publication 28 June 2000)

The growth of microcrystalline silicon, μc-Si, films has been studied by infrared spectroscopy and x-ray diffraction. Thin films of various thickness have been prepared from SiH_4–H_2 mixtures by electron-cyclotron resonance chemical vapor deposition. Two structural transitions were observed during film growth. The first transition at a critical thickness of $d_{ac}=9$ nm manifested itself by a change from an initially amorphous growth to polycrystalline growth. The second structural transition was related to an increasing amount of silicon grains of preferred orientation with (110) lattice planes parallel to the substrate. The population of such (110)-oriented grains N_{110} was found to become dominant at about $d_{110}=310$ nm, which may be considered as a second critical thickness above which the film exhibits a (110) fiber texture. The increase of N_{110} with increasing thickness follows a $d^{1/6}$ dependence. The effect is understood in terms of an interplay between etching and deposition during growth. © *2000 American Institute of Physics.* [S0021-8979(00)08719-3]

INTRODUCTION

The growth of thin microcrystalline silicon films on large-area substrates is a question of key interest for next-generation solar cells[1] and other optoelectronic devices.[2] The microcrystalline Si phase, μc-Si, is considered to be more favorable for certain applications than the related hydrogenated amorphous silicon, a-Si:H, mainly due to an improved stability and larger electronic mobilities.[3] For photovoltaic applications, thin film growth should be performed at temperature significantly lower than the softening temperature of glass and with a high deposition rate. Thin films, as obtained by such processes, generally consist of small silicon crystallites exhibiting grain sizes in the 10–100 nm range.

The efficiency of solar cells made from μc-Si is generally considered to be strongly influenced by grain boundaries and grain boundary defects. Therefore, it is concluded that the efficiency is controlled by the degree of crystallinity and various techniques like Raman spectroscopy, x-ray diffraction (XRD), scanning and transmission electron microscopy (TEM) have been applied to investigate its microstructure. The Raman spectrum of μc-Si films with a high degree of crystallinity exhibits a strong band at around 520 cm^{-1}, which is the longitudinal/transversal optical phonon peak of single-crystalline Si. On the other hand, the intensity at around 480 cm^{-1}, where the signal of a thin a-Si film would peak, is only small, indicating a small amount of any remaining amorphous phase. Highly crystalline films often exhibit a preferred orientation, i.e., texture, where crystallites with (110) lattice planes are preferably oriented parallel to the substrate surface.[4–10] Due to the high symmetry of the diamond structure many reflections like the (110) in the x-ray powder diffractogram of Si are forbidden, and the texture can just be monitored by observation of the (220) intensity. For vapor-based processes having an axially symmetric deposition configuration the preferred orientation may be assumed to be of the same symmetry, which is named a fiber texture.[11] In order to study the evolution of structural properties in μc-Si we have prepared a set of samples of varying thickness by electron-cyclotron resonance chemical vapor deposition (ECRCVD) and investigated their structure by infrared spectroscopy and x-ray diffraction.

EXPERIMENT

Thin μc-Si films were deposited from silane–hydrogen mixtures at a substrate temperature of 325 °C with an ECR plasma-enhanced CVD system. The plasma is produced by resonant absorption of a 2.45 GHz microwave in a 875 G magnetic field. The system has been described in detail before.[12] Gas flow rates amounted to 4 and 90 sccm for SiH_4 and H_2, respectively, and the pressure in the deposition chamber was regulated by the throttle valve to 7 mTorr. The base pressure prior to deposition was less than 10^{-7} Torr and the power of the plasma-exciting microwave amounted to 1000 W. This set of deposition parameters has been identified by a preceding factorial analysis campaign[13] aimed at the optimization of crystallinity of μc-Si films as prepared by this technique.[14] Depositions were performed under floating bias conditions on Mo-coated Corning 1737F glass, the surfaces of which were electrically connected to the susceptor. A thickness series was prepared by variation of the deposition time (15, 30, 60, 120, and 240 min) with otherwise unchanged conditions. Film thicknesses d were derived from interference maxima in the Fourier transform infrared (FTIR) reflection spectrum measured with a Perkin Elmer 2000 FTIR for wave numbers 400–8000 cm^{-1}. The refractive index of crystalline silicon $n_{Si}=3.42$ was used for the evaluation of d. The obtained values could well be fitted as a function of time t by the linear relationship $d=a+bt$, with parameters $a=48(5)$ nm and $b=12.66(3)$ nm/min. The small errors certify a high degree of consistency within the

[a]Electronic mail: birkholz@hmi.de

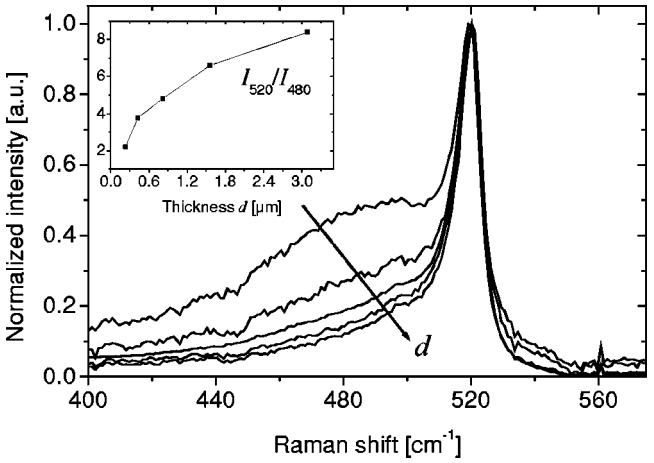

FIG. 1. Raman spectra of μc-Si samples measured by exciting with a HeNe laser line. Parameter is the thickness d of the films. Intensities are normalized to the peak intensity at 520 cm^{-1}. The inset displays the dependence of the intensity ratio I_{520}/I_{480} on d.

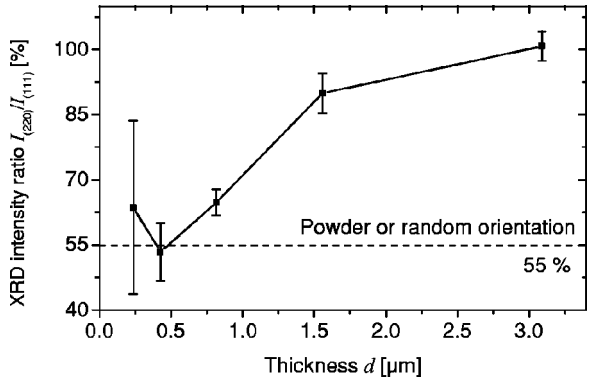

FIG. 2. Ratio of XRD reflection intensity I_{220}/I_{111} vs film thickness measured in θ–2θ geometry. Intensities have been corrected for finite thickness of the sample, so the values may directly be compared with those of an infinitely thick powder. The connecting line is a guide to the eye. Broken line at 55% indicates the ratio for a random orientation of grains as observed for a powder.

data set. An interesting conclusion may be drawn from the fact that $a>0$ was found. This suggests that a phase other than crystalline silicon was grown initially, which has a higher index of refraction, $n>n_{\mathrm{Si}}$. The large value of the constant a in comparison to the linear coefficient b, moreover, can only be understood by assuming the growth of the initial layer to be faster than the growth of the rest of the film.

Raman spectra were measured with a Dilor/ISA LabRAM 010 system using two exciting laser lines, the 632.8 nm line of a HeNe laser and the 457.9 nm line of an Ar ion laser. The spectra taken with the red HeNe line were normalized with respect to the maximum intensity at around 520 cm^{-1}, Fig. 1. The thinner films exhibit a second local maximum at 480 cm^{-1}, which clearly indicates the presence of an a-Si:H phase within the samples. The signal amplitude at this wave number decreases with increasing thickness and almost vanishes for the thickest sample. The inset in Fig. 1 shows the ratio of Raman intensities at 520 and 480 cm^{-1} $(I_{520}/I_{480})_{\mathrm{red}}$ versus film thickness. This ratio is usually taken as a figure of merit for the degree of crystallinity. $(I_{520}/I_{480})_{\mathrm{red}}$ increases from 2.2 to 8.4 with increasing film thickness. We also determined the $(I_{520}/I_{480})_{\mathrm{blue}}$ ratio from spectra that were excited with the Ar ion laser line and found a constant value of about 12 for all film thicknesses. This different behavior has to be understood by the difference in penetration depth which amount in μc-Si to about 300 nm for the red and 50 nm for the blue laser line.[15] The results from both IR and Raman spectroscopy can consistently be explained by assuming that the initial growth yield amorphous silicon and that after a certain thickness crystalline growth takes over. This observation seems to be different from an earlier result obtained on μc-Si films deposited by ECRCVD using a different set of deposition parameters.[16] In this work a thickness dependence in the so-called crystalline fraction as derived from the deconvolution of Raman spectra could not be detected and it was stated that the film had been grown without an amorphous silicon interlayer. It thus appears that the thickness of the initial amorphous layer may sometimes be too small to be detected or may be influenced by the choice of deposition parameters.

X-ray diffractograms were measured in symmetric θ–2θ geometry. A Bruker D8 Advance diffractometer was used which was equipped with a Göbel mirror for parallel beam diffraction[17] and operated with Cu $K\alpha$ radiation ($\lambda_{\alpha 1}$ $=154.06$ pm). Diffractograms were recorded with and without rotating the sample around the substrate normal, but no dependence on the rotation angle ϕ was detected. The recorded Bragg reflections could well be fitted by Lorentzian line profiles and integrated intensities were calculated from the line shape parameters. These measured intensity values $M_{(hkl)}$ were corrected for finite absorption by dividing $I_{(hkl)}=M_{(hkl)}/A$ with a thickness-dependent absorption factor $A=(1-\exp(-2\mu d/\sin\theta))$,[18] where $\mu=148\,\mathrm{cm}^{-1}$ accounts for the x-ray absorption coefficient for Si under Cu $K\alpha$ radiation,[19] and θ stands for the Bragg angle. Figure 2 displays the corrected intensity ratio $I_R=I_{(220)}/I_{(111)}$ for the first two Bragg reflections (111) and (220) as a function of thickness, which—after absorption correction—may be directly compared with the value for an infinitely thick powder $(d\gg 1/\mu)$. The broken line at 55% represents the expected ratio $I_{(220)}/I_{(111)}$ for a Si powder consisting of randomly oriented grains, according to the Joint Committee on Powder Diffraction Standards card 27-1402.[20] It can clearly be seen that the concentration of grains having (110) planes oriented parallel to the substrate increases with d. For the thickest sample the intensity of the (110) reflection is enhanced by a factor of about 2 compared to the powder case with random orientation. A comparable plot was obtained for the ratio $I_{(220)}/I_{(311)}$ (not shown here). We conclude that an axially symmetric texture, i.e., fiber texture, has developed in the $\langle 110\rangle$ direction for the thicker films. Moreover, it is seen from the figure that the (110) fiber texture evolved with increasing film thickness. This observation implies that there is a selection process active during the deposition process, favoring the crystal growth of (110)-oriented grains.

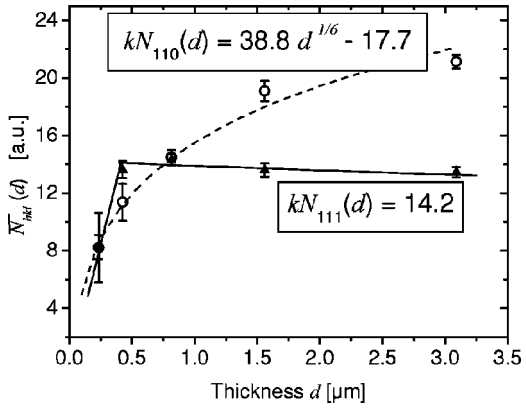

FIG. 3. Average population $\overline{N}_{hkl}(d)$ of (111) and (110) grains oriented parallel to the substrate plane. Dots and error bars account for experimental data, while the solid and broken lines have been calculated with the depth-dependent population functions given in the insets.

DISCUSSION

In order to accurately elucidate the critical thickness, for which the (110) texture starts to dominate, we carefully analyzed the measured XRD intensities. The integral intensity of a Bragg reflection from a thin film is given by

$$I_{hkl}(d) = k \cdot L \cdot m \cdot D \cdot \overline{N}_{hkl}(d) \cdot A, \tag{1}$$

where k is a constant independent of θ, hkl, and d. L denotes the Lorentz-polarization factor, m the multiplicity of the reflex, and D the temperature factor. L, m, and D are well defined functions, into which either θ or known material parameters enter [isotropic Debye–Waller factor $B_{\mathrm{Si}} = 0.53\ \text{Å}^2$ (Ref. 21)]. $\overline{N}_{hkl}(d)$ is the average number of grains that reflect into the detector. It is given by the weighted integral over the depth-dependent population of grains $N_{hkl}(d)$

$$\overline{N}_{hkl}(d) = A^{-1} \int_0^d N_{hkl}(z) \exp(-2\mu z/\sin\theta) dz \tag{2}$$

with the weight function accounting for the sample's absorption. In the case of random orientation of grains all N_{hkl} become equal and independent of thickness. We have calculated the quantity $k\overline{N}_{hkl}(d)$ for both the (111) and the (220) reflections by dividing $I_{hkl}(d)$ by $L \cdot m \cdot D \cdot A$. The depth-dependent population functions $N_{hkl}(d)$ were then obtained by solving the integral Eq. (2) through fitting with reliable model functions like polynomials and rational functions. The choice of appropriate model functions was restricted by the fact that only five data points were available for the fitting procedure. The results are given in Fig. 3, where dots and error bars represent experimental data and the solid and broken lines show calculated values of $k\overline{N}_{hkl}(d)$ when the fitted population functions $N(d)$ are inserted. For an interpretation of the figure, the depth-dependent distribution function $N(d)$ should not be confused with the average population $\overline{N}_{hkl}(d)$, see Eq. (2). On the one hand, it may be seen from the figure that the population of (111)-oriented grains suddenly increases at some 100 nm and then remains at a constant value, $kN_{111}(d) = 14.2$. On the other hand, the population of (220) or, equivalently, (110) grains follows the relation $kN_{110}(d) = 38.8d^{1/6} - 17.7$ (d in μm). Two critical thickness values may be inferred from these functions. First, it follows from $N_{110} = 0$ a value of $d_{\mathrm{ac}} = 9$ nm. For this thickness N_{110} becomes larger than zero, i.e., takes physical meaningful values. The thickness d_{ac} is accordingly identified with the critical thickness for which the amorphous–crystalline transition occurs. Second, a value of $d_{110} = 310$ nm is derived from $N_{110} = N_{111}$. This height is associated with the thickness, where the population of (110) grains exceeds that of (111), i.e., the point where the film starts to exhibit a (110) fiber texture. It should be emphasized that the (110) population starts to increase immediately after the amorphous–crystalline transition and that its increase follows the same $d^{1/6}$ dependence before and after it has exceeded the population of (111) grains.

The presented results from both IR spectroscopy and x-ray diffraction suggest the following picture. The initial growth phase is unambiguously associated with the growth of amorphous silicon. This result is fully compatible with previous TEM studies of plasma enhanced (PE) CVD-grown μc-Si films[22–24] where an amorphous layer of some 10 nm thickness was obtained during the initial growth phase. In a second growth phase, which starts approximately at $d_{\mathrm{ac}} = 10$ nm above the substrate–film interface, crystalline silicon grains begin to grow. The amorphous–crystalline transition has been observed in various studies to occur with deposition techniques such as low pressure and PECVD, and hot-wire CVD.[9,22–25] We are presenting the same result obtained by an ECRCVD process. It thus appears that the structural phase transition during growth is as an inherent property of the growth of μc-Si films on foreign substrates at low temperatures. It has to be added, however, that the critical thickness of the amorphous interlayer can be reduced by depositing it in a high hydrogen dilution regime.[9,26] We showed, in addition, that the crystalline growth is associated with a steady increase of (110)-oriented grains with the concentration of (111)-oriented grains remaining constant. The increase of the (110) population N_{110} follows a $d^{1/6}$ dependence for the thin films prepared by ECRCVD at low temperatures in this study.

One possible explanation for the occurrence of fiber textures is related to the minimization of elastic energy due to stress or strain imposed on the film through its interaction with the substrate. In the case of low-temperature deposition of high-melting point elements the biaxial stress model generally applies.[27] The model predicts a certain preferred orientation of grains determined by the elastic constants of the material under consideration. If the biaxial stress model is applied to the growth of Si films and the elastic constants of silicon are inserted[27] it turns out that a (111) fiber texture would be more favorable than a (110) fiber structure. This is in contradiction to the experimental observations. An alternative explanation is based on growth velocity differences of silicon lattice planes along distinct crystallographic directions. Such a model has been put forward by Kamins and Cass[4] and later adopted by Bisaro *et al.*[5] This explanation would only apply if (110) grains would increase in size with increasing film thickness. In order to elucidate this question, grain sizes were determined from the line broadening of

XRD reflections under the assumption that line broadening effects due to strain and lattice faults like twinning and stacking faults[28] may be neglected. Average vertical dimensions in the 21–26 nm range were then obtained for (110)-oriented grains, which turned out to be independent of depth. Both models thus lead to either wrong predictions or contradictions to other observations and, therefore, have to be excluded to account for the effect. Kakinuma has proposed a comprehensive interpretation of preferred orientation in thin silicon films.[6] Next to preferential nucleation and the concept of surface free energy he emphasized the significance of the microscopic geometry of the growing surfaces and the surface kinetics. This latter point is associated with the hydrogen termination of the silicon surface and the effects of surface etching. It is within this framework that we understand the observed evolution of fiber texture.

We propose that the evolution of texture may arise from the interplay of growth of new crystalline nuclei and their etching back. According to this model the growth of (110)-oriented nuclei is enhanced if it occurs upon other (110) grains. The orientation of grains of the sublayer would then influence the orientation of the actually forming layer. However, a second—decelerating—mechanism must be active, since one would observe a much steeper increase as described by $d^{1/6}$ of the (110) population. This other mechanism which decelerates (110) growth could be due to the etching back which inevitably occurs for all freshly formed grains exposed to the gas-plasma phase. The etching of silicon is well known to be strongly anisotropic, i.e., to depend on the crystallographic face which is actually etched off. In the case of CVD processes highly reactive hydrogen species permanently impinge on the substrate at a much higher rate than silicon species. Therefore, we argue that the (110) orientation of the growing nuclei is determined by the orientation of the sublayer which—in combination with etching—causes the $d^{1/6}$ dependence of the evolution of fiber texture. This interpretation is in accordance with the explanation presented for a (100) texture that has been observed for μc-Si films grown from SiF_4–H_2 mixtures.[10] In that case, the active etching species are different than in SiH_4–H_2 mixtures causing different etching velocities of crystallographic lattice planes. More work on the growth process of μc-Si films is clearly necessary to investigate in how far the $d^{1/6}$ dependence as found here for ECRCVD can be influenced by the deposition technique or tailored by process conditions.

CONCLUSION

We have investigated the evolution of structural properties of thin μc-Si films grown by ECRCVD at low temperatures. The initially grown layer on a foreign substrate turned out to consist of amorphous silicon. This is in accordance with previous growth studies that used other deposition techniques. At a critical thickness d_{ac} of about 10 nm the growth mode changes and crystalline Si grains are formed. From this point the population N_{110} of (110)-oriented grains increases according to a $d^{1/6}$ dependence. At a second critical thickness d_{110} of about 310 nm N_{110} exceeds N_{111} and the film starts to exhibit a (110) fiber texture. It has been successfully attempted to solve for the depth-dependent population function of (110)-oriented grains from XRD intensities. The evolution of preferred orientation is interpreted by the interplay between nucleation and etching of μc-Si grains.

ACKNOWLEDGMENTS

The authors would like to thank F. Fenske for molybdenum deposition on Corning glass, G. Keiler, J. Krause, and M. Schmidt for technical assistance, and P. Müller for stimulating discussions. This work was partially supported by the Bundesministerium für Wirtschaft (Contract No. 329773).

[1] A. Shah, P. Torres, R. Tscharner, N. Wyrsch, and H. Keppner, Science **285**, 692 (1999).
[2] Y. Hamakawa, Appl. Surf. Sci. **142**, 215 (1999).
[3] R. H. Bube, *Photovoltaic Materials* (Imperial College Press, London, 1998), Vol. 1, p. 57.
[4] T. I. Kamins and T. R. Cass, Thin Solid Films **16**, 147 (1973).
[5] R. Bisaro, J. Maraino, N. Proust, and K. Zellama, J. Appl. Phys. **59**, 1167 (1986).
[6] H. Kakinuma, J. Vac. Sci. Technol. A **13**, 2310 (1995).
[7] Y. Sun, T. Miyasato, and J. K. Wigmore, Appl. Phys. Lett. **70**, 508 (1997).
[8] R. Nozawa, H. Takeda, M. Ito, M. Hori, and T. Goto, J. Appl. Phys. **81**, 8035 (1997).
[9] J. K. Rath, F. D. Tichelaar, H. Meiling, and R. E. I. Schropp, Mater. Res. Soc. Symp. Proc. **507**, 879 (1988).
[10] T. Kamiya, K. Nakahata, A. Miida, C. M. Fortmann, and I. Shimizu, Thin Solid Films **337**, 18 (1999).
[11] H.-J. Bunge, Z. Metallkd. **76**, 457 (1985).
[12] P. Müller, E. Conrad, T. R. Omstead, and P. Kember, *13th EC Photovoltaic Solar Energy Conference* (Stephens 1995), p. 1742.
[13] S. Wolf and R. N. Tauber, *Silicon Processing for the VLSI Era* (Lattice, Sunset Beach, CA, 1986), Vol. 1, p. 618–646.
[14] M. Birkholz, E. Conrad, K. Lips, B. Selle, I. Sieber, S. Christiansen, and W. Fuhs, Mater. Res. Soc. Symp. Proc. **609**, () (in press).
[15] M. Schmidt, R. Krankenhagen, M. Poschenrieder, W. Henrion, I. Sieber, S. Grebner, S. Koynov, and R. Schwarz, J. Non-Cryst. Solids **198–200**, 923 (1996).
[16] I. Kaiser, N. Nickel, W. Fuhs, and W. Pilz, Phys. Rev. B **58**, R1718 (1998).
[17] M. Schuster and H. Göbel, Adv. X-Ray Anal. **39**, 1 (1996).
[18] M. Birkholz, S. Fiechter, A. Hartmann, and H. Tributsch, Phys. Rev. B **43**, 11 926 (1991).
[19] D. C. Creagh and J. H. Hubbel, in *International Tables for Crystallography*, Vol. C, edited by A. J. C. Wilson (Kluwer, Dorderecht, 1992), p. 189.
[20] Natl. Bur. Stand. (US), Monogr. **13**, 35 (1976).
[21] H. X. Gao and L.-M. Peng, Acta Crystallogr., Sect. A: Found. Crystallogr. **55**, 926 (1999).
[22] S.-i. Ishihara, D. He, and I. Shimizu, Jpn. J. Appl. Phys., Part 1 **33**, 51 (1994).
[23] I. Sieber, I. Urban, I. Dörfel, S. Koynov, R. Schwarz, and M. Schmidt, Thin Solid Films **276**, 314 (1996).
[24] C. Ross, J. Herion, and H. Wagner, J. Non-Cryst. Solids (in press).
[25] G. Harbeke, L. Krausbauer, E. F. Steigmeier, A. E. Widmer, H. F. Kappert, and G. Neugebauer, J. Electrochem. Soc. **131**, 675 (1984).
[26] J.-H. Zhou, K. Ikuta, T. Yasuda, T. Umeda, S. Yamasaki, and K. Tanaka, Appl. Phys. Lett. **71**, 1534 (1997).
[27] A. Segmüller and M. Murakami, in *Analytical Techniques For Thin Films*, edited by K. N. Tu and R. Rosenberg (Academic, Boston, MA, 1988), pp. 143–200.
[28] B. E. Warren, *X-Ray Diffraction* (Addison-Wesley, Reading, MA, 1969).